

Proceeding Paper

Graphitic Carbon Nitride-Supported L-Arginine: Synthesis, Characterization, and Catalytic Activity in Multi-Component Reactions[†]

Fatemeh Bijari, Maryam Talebi, Hossein Ghafuri *, Zeinab Tajik and Peyman Hanifehnejad

Catalysts and Organic Synthesis Research Laboratory, Department of Chemistry, Iran University of Science and Technology, Tehran 16846-13114, Iran

* Correspondence: ghafuri@iust.ac.ir

[†] Presented at the 26th International Electronic Conference on Synthetic Organic Chemistry, 15–30 November 2022; Available online: <https://ecsoc-26.sciforum.net/>.

Abstract: Graphitic carbon nitride-supported L-arginine (g-C₃N₄@L-arginine) has been prepared as a heterogeneous catalyst for synthesizing heterocyclic compounds such as pyranopyrazole and acridinedione derivatives. High efficiency, short reaction time, and easy separation are significant features that are reasons for using g-C₃N₄@L-arginine as a catalyst in one-pot multicomponent reactions. Synthesized nanocatalyst was detected by numerous analyses, such as FE-SEM (Field Emission Scanning Electron Microscopy), EDX (Energy Dispersive X-ray spectroscopy), XRD (X-Ray Diffraction analysis), TGA (Thermo Gravimetric Analysis), and FT-IR (Fourier Transform Infrared Spectroscopy). G-C₃N₄@L-arginine nanocatalyst was reused 5 times in the reaction with no apparent decrease in reaction yield, which shows acceptable recyclability.

Keywords: g-C₃N₄-pyranopyrazole; acridinedione; multi-component; L-arginine



Citation: Bijari, F.; Talebi, M.; Ghafuri, H.; Tajik, Z.; Hanifehnejad, P. Graphitic Carbon Nitride-Supported L-Arginine: Synthesis, Characterization, and Catalytic Activity in Multi-Component Reactions. *Chem. Proc.* **2022**, *12*, 50. <https://doi.org/10.3390/ecsoc-26-13708>

Academic Editor: Julio A. Seijas

Published: 18 November 2022

Publisher's Note: MDPI stays neutral with regard to jurisdictional claims in published maps and institutional affiliations.



Copyright: © 2022 by the authors. Licensee MDPI, Basel, Switzerland. This article is an open access article distributed under the terms and conditions of the Creative Commons Attribution (CC BY) license (<https://creativecommons.org/licenses/by/4.0/>).

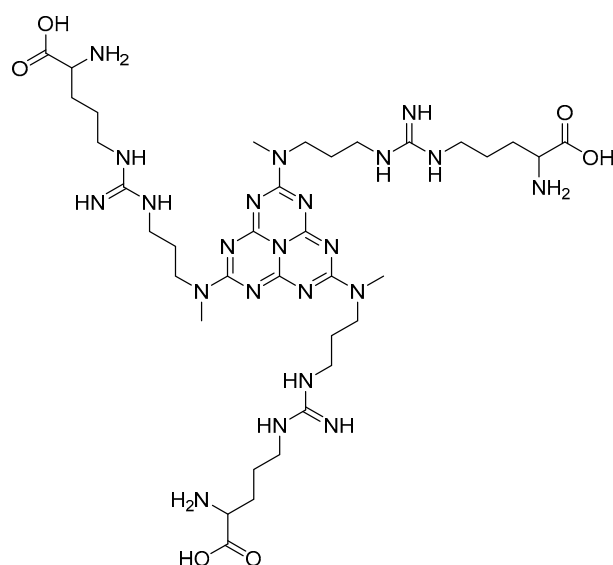
1. Introduction

In the last decades, heterogeneous catalysts have been noticed because of large-scale production and selective product formation [1,2]. G-C₃N₄ is a widely used support for catalytic entities due to high physical and thermal stability, low density, versatile performance, and recyclability. Moreover, the preparation of g-C₃N₄ is mostly performed by Cyanamid, urea, dicyanamide, melamine, and thiourea as the precursor [3]. To increase the efficiency of the catalytic performance of g-C₃N₄ in organic reactions, it is suggested to modify it with organic compounds [4–8].

Significantly, L-arginine is a semi-essential amino acid in living organisms [9], while the guanidine group in L-arginine is the precursor for synthesizing nitrogen derivatives. Using L-arginine with g-C₃N₄ as a catalyst support can decrease the cost and toxicity. Among other benefits of composite productions with L-arginine, it should be mentioned that making composite with this amino acid can increase thermal stability and molar heat capacities. Although, on the other hand, it can reduce the thermal expansion coefficient. Moreover, the utilization of composites is one of the best ways for synthesizing heterocyclic compounds [10–13], while heterocyclic compounds have been considered essential groups of organic materials. In addition, they have biological activities which could be effective in the treatment of different diseases. What makes these compounds more important than others is their application in various fields such as medicines, veterinary products, disinfectants, and antioxidants. There are several ways of synthesizing heterocyclic compounds including the multi-stages and one-pot multicomponent reactions. Lately, projects indicate that multicomponent reactions could be the best way for preparing heterocyclic compounds.

Multicomponent reactions have been mostly used for producing heterocyclic compounds because of their advantages including step efficiency, atom economy, and reducing the waste production [14–18]. Pyranopyrazoles are nitrogen-containing heterocyclic compounds with various properties such as anti-cancer, anti-inflammatory, anti-bacterial, antioxidant, and antihypertensive. Knoevenagel condensation, Micheal addition, and cyclization are the main procedures for making pyranopyrazoles derivatives. Various catalysts can be utilized to prepare pyranopyrazole and its derivatives by multicomponent reactions such as cetyltrimethylammonium chloride (CTACl), montmorillonite K10, agave leaf ash, cytosine@MCM-41, Et₃N, and PTSA [19–24].

Other heterocyclic compounds with biological activities that can be produced with multicomponent reactions are Acridinedione derivatives [25]. They are nitrogen-mediated heterocyclic compounds with a vast spectrum of pharmaceutical and biological activities, namely anti-tumor, SIRT1 inhibitors, anticancer, and antimicrobial agents [26–29]. There are different precursors such as heterogeneous catalysts for preparing acridinedione, including f-MWCNT, Amberlyst -15, CTAB, and Proline [30–33]. Usually, recent methods can cover problems of the latest projects such as harsh conditions, long reaction time, and using toxic solvents. Therefore, new methods for synthesizing pyranopyrazole and acridinedione derivatives are a critical challenge in chemistry society. Consequently, in this research, we have synthesized g-C₃N₄@L-arginine nanocomposite and applied it as a catalyst in the synthesizing pyranopyrazole and acridinedione derivatives in a high yield. The schematic of g-C₃N₄@L-arginine is shown in Scheme 1.



Scheme 1. Schematic of g-C₃N₄@L-arginine.

2. Experimental

2.1. Materials

All chemicals were obtained from Sigma–Aldrich and Merck companies. Many analyses have been performed, including Fourier Transform Infrared Spectroscopy (FT-IR), which was recorded by Tensor27 for detecting functional groups of products; Thermal Gravimetric Analysis (TGA) under argon atmosphere was taken by STA 504, which displayed the thermal stability of nanocatalyst; Nuclear Magnetic Resonance (NMR) with Varian-Inova 500 MHz, X-Ray Powder Diffraction (XRD) was performed by Dron-8; Energy-Dispersive X-ray (EDX) Numerix DXP–X10P was employed for indicating the existence of elements of synthesized nanocatalyst; and Field Emission Scanning Electron Microscopy (FE-SEM) with TESCAN-MIRA III was used for displaying the morphology of synthesized nanocatalyst.

2.2. Preparation of Bulk C_3N_4 and $g-C_3N_4$

Melamine is precursor for preparing bulk carbon nitride, which was heated to 550 °C temperature by the ramp of 2.5 °C.min⁻¹ in a furnace for 4 h. Eventually, a yellow powder was formed. Then, for preparing $g-C_3N_4$, 1.0 g bulk C_3N_4 was stirred with 20 mL H_2SO_4 at 90 °C for 5 h. Afterward, the mixture was diluted with 200 mL ethanol and stirred at room temperature for 2 h. Then, the mixture was dispersed in 100 mL water/isopropanol (1:1), sonicated for 6 h, and centrifuged to obtain $g-C_3N_4$.

2.3. Preparation of $g-C_3N_4@L$ -Arginine

A total of (1.0 g) $g-C_3N_4$ with (20.0 mL) dry toluene was dispersed. Then, (2.0 mL) 1,3-dibromopropane was poured into the final mixture and refluxed for 24 h under an N_2 atmosphere. After filtration and washing with ethyl acetate, the product was dried at room temperature. The final product was dissolved in a mixture of water and methanol (1:1). Then, each of the following ingredients was added, respectively: L-arginine (1 mmol), K_2CO_3 (1.0 mmol), and NaI (1.0 mmol). Afterward, it was stirred for 24 h at room temperature, washed with water and methanol, then dried at 80 °C.

2.4. Synthesizing Acridinedione Derivatives

A mixture of dimedone (2 mmol), ammonium acetate (1 mmol), aromatic aldehyde (1 mmol), ethanol (5 mL), and catalyst (0.18 mol %) was poured into a flask and refluxed for the appropriate time. The reaction progress was monitored by TLC. After completion of the reaction, the mixture was cooled to room temperature, the catalyst was filtered, and the intended product was obtained by crystallization.

2.5. Synthesizing Pyranopyrazole Derivatives

A mixture of aldehyde (1.0 mmol), ethyl acetoacetate (1.0 mmol), hydrazine hydrate (1.0 mmol), malononitrile (1.0 mmol), catalyst (0.18 mol %), and ethanol (2.0 mL) was poured into a 25 mL round bottom flask and refluxed for the appropriate time. The reaction progress was monitored by TLC. After completion of the reaction, the mixture was cooled to room temperature, the catalyst was filtered, and the intended product was obtained by crystallization.

3. Results and Discussion

FT-IR spectra of a) $g-C_3N_4$, b) modified $g-C_3N_4$, and c) $g-C_3N_4@L$ -arginine are shown in Figure 1. In Figure 1a, there is a broad peak around 3000–3300 cm^{-1} for N-H group stretching vibrations which is related to H-bonding or actually the existence of the OH group of water adsorption by $g-C_3N_4$ nanosheets. Figure 1b demonstrates the modified $g-C_3N_4$ nanosheets around 3000–2800 cm^{-1} which is related to C-H stretching vibrations. In Figure 1c, stretching vibrations of C=O and C-O were shown at (1705 cm^{-1}) and (1320–1210 cm^{-1}), respectively. A peak around 1602 cm^{-1} indicates carbon double bond nitrogen and its stretching vibrations. Values of 1303 and 1082 cm^{-1} are related to the C-N bond stretching vibrations which are formed from triazine and N-H groups. The C-N stretching vibrations in the ring are significantly revealed at 1448 and 1379 cm^{-1} . A value of 786 cm^{-1} was shown because of tri-s-triazine vibrations. According to the mentioned peaks, $g-C_3N_4@L$ -arginine was synthesized [3,4].

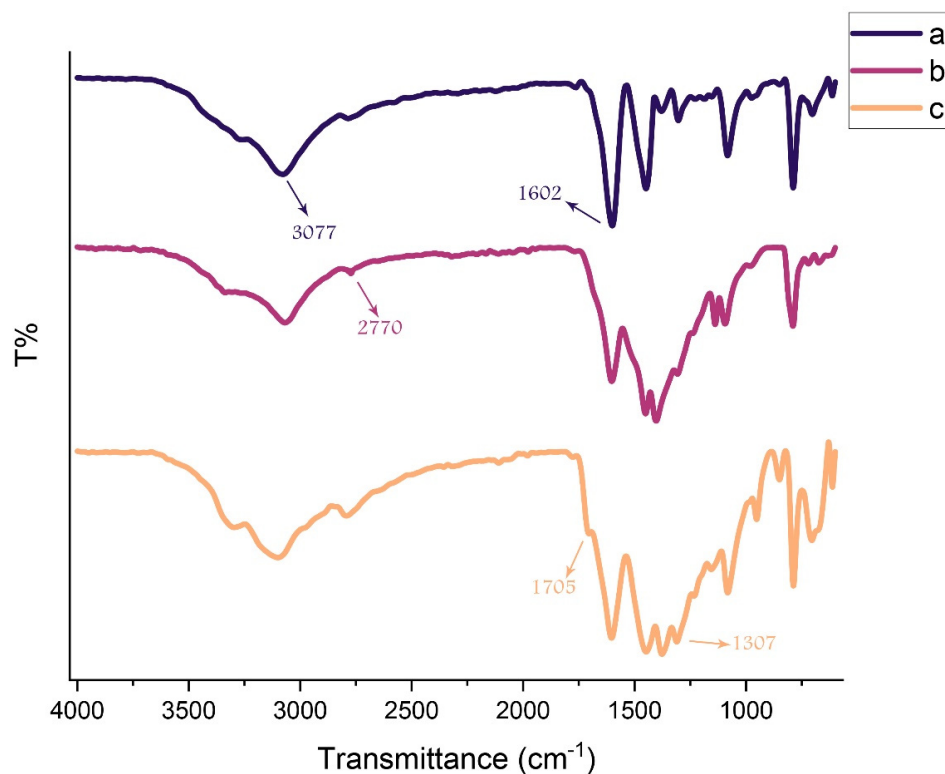


Figure 1. FT-IR spectra of (a) $g\text{-C}_3\text{N}_4$, (b) modified $g\text{-C}_3\text{N}_4$, and (c) $g\text{-C}_3\text{N}_4@L\text{-arginine}$.

EDX analysis determined the presence of elements in (a) $g\text{-C}_3\text{N}_4$ nanosheets, (b) modified $g\text{-C}_3\text{N}_4$, and (c) $g\text{-C}_3\text{N}_4@L\text{-arginine}$. Nitrogen and Carbon elements in nanosheet $g\text{-C}_3\text{N}_4$ are visible in Figure 2a. In Figure 2b, the existence of the Br element would confirm the modification of $g\text{-C}_3\text{N}_4$ nanosheets. Moreover, Figure 2c revealed the presence of carbon, nitrogen, and oxygen, which confirm the synthesizing of $g\text{-C}_3\text{N}_4@L\text{-arginine}$.

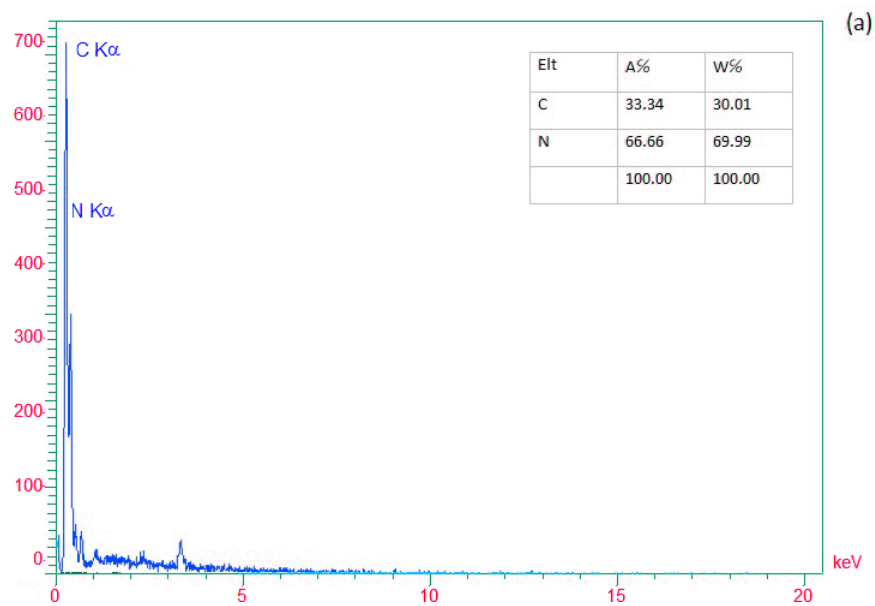


Figure 2. Cont.

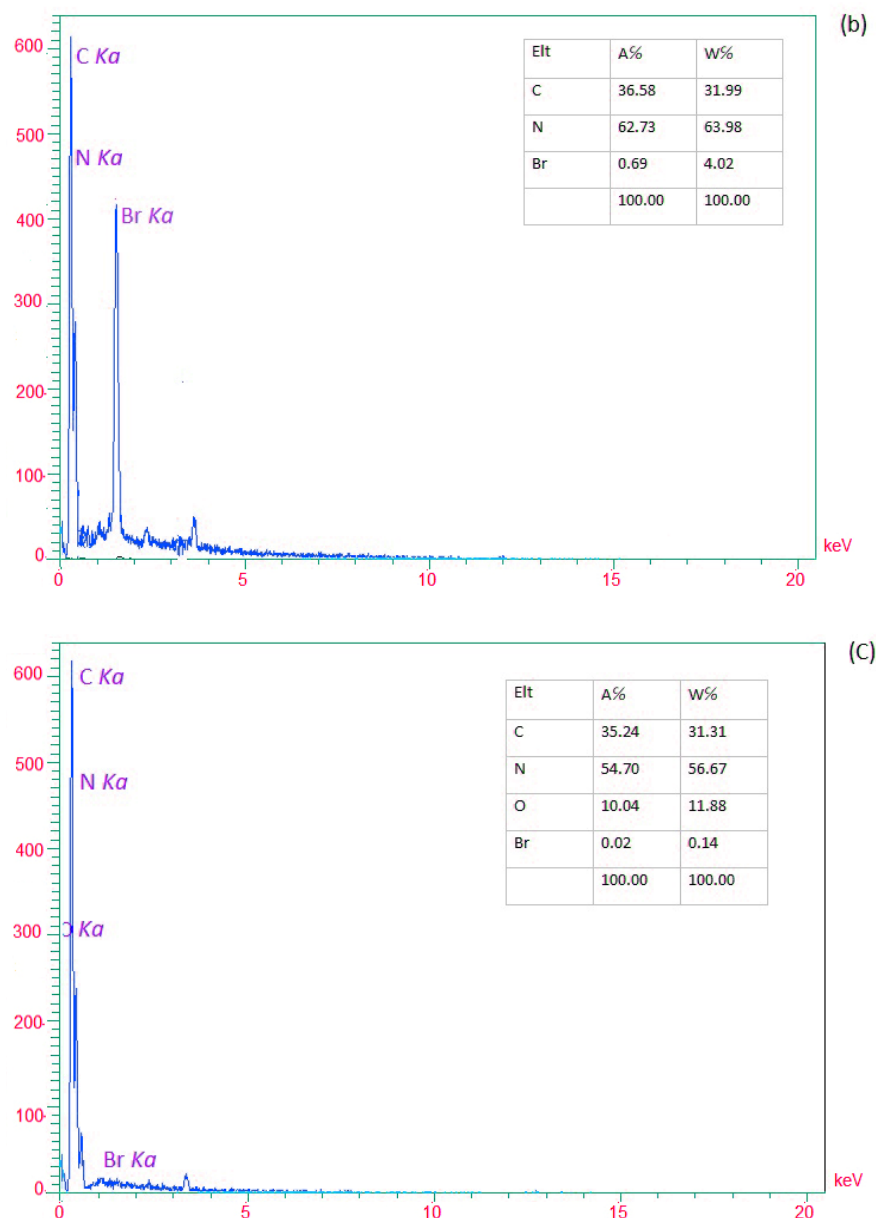


Figure 2. EDX spectra of (a) $g\text{-C}_3\text{N}_4$ nanosheets, (b) modified $g\text{-C}_3\text{N}_4$, and (c) $g\text{-C}_3\text{N}_4@L\text{-arginine}$.

The morphology of $g\text{-C}_3\text{N}_4@L\text{-arginine}$ nanocatalyst was studied by FE-SEM analysis in two scales (200 nm and 1 μm). Graphitic and nanosheet properties of C_3N_4 are apparent based on Figure 3. It can be concluded that the $g\text{-C}_3\text{N}_4@L\text{-arginine}$ nanocatalyst synthesizing has been successfully performed by observing the $g\text{-C}_3\text{N}_4$ surface roughness.

The XRD of $g\text{-C}_3\text{N}_4$ nanosheets and $g\text{-C}_3\text{N}_4@L\text{-arginine}$ have been shown in Figure 4a,b. XRD pattern of nanosheet $g\text{-C}_3\text{N}_4$ in part (a) indicates the diffraction angles of $2\theta = 15.96^\circ$ and $2\theta = 27.69^\circ$, which approve the synthesizing of $g\text{-C}_3\text{N}_4$ [34]. Diffraction angles of $2\theta = 30.97^\circ$, 23.60° , 12.21° , 10.85° , 6.07° in XRD pattern part (b) indicate the L-arginine on the surface of $g\text{-C}_3\text{N}_4@L\text{-arginine}$ (JCPDS card no. 00-004-0180).

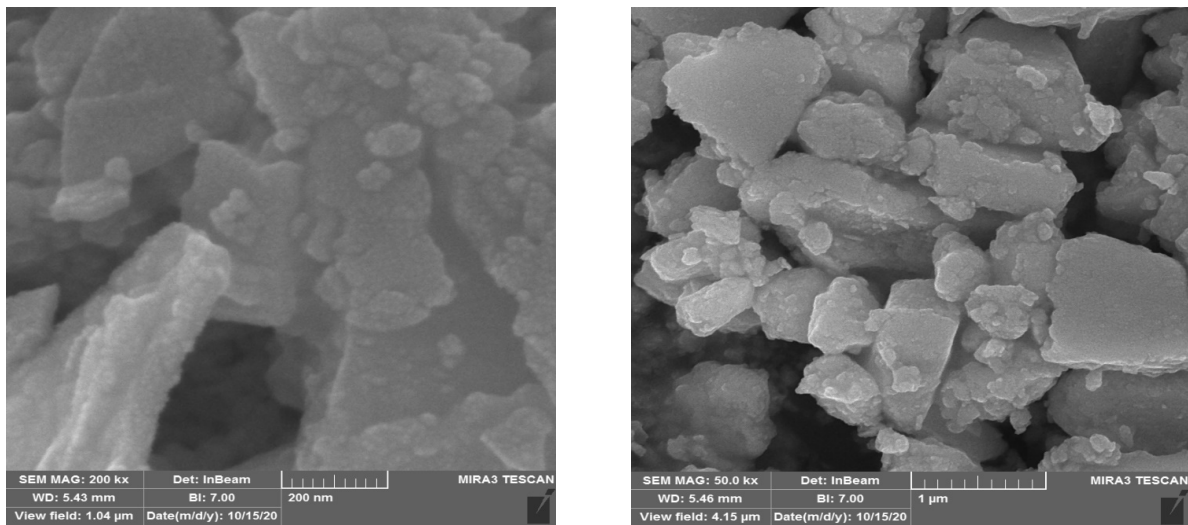
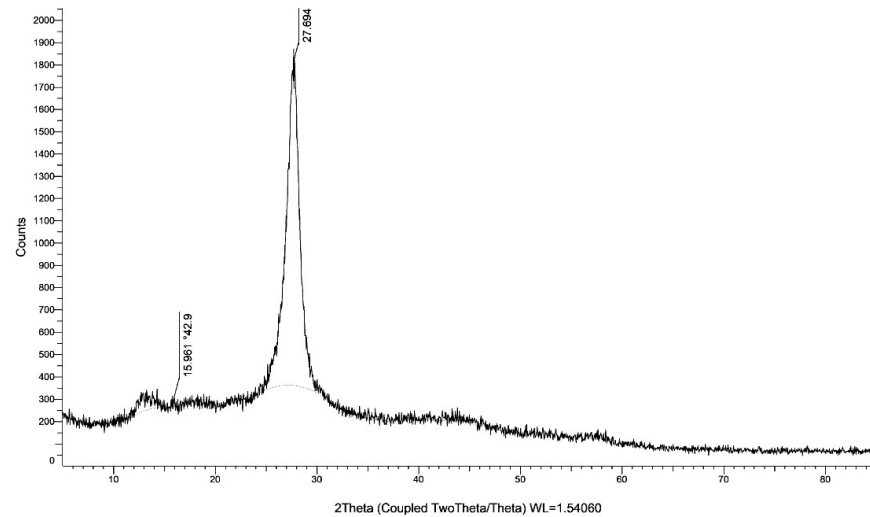
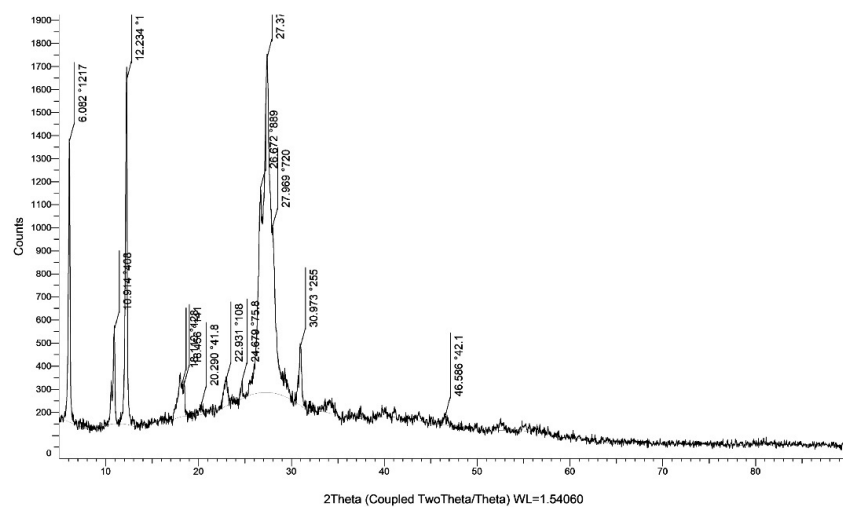


Figure 3. FE-SEM images of g-C₃N₄@L-arginine.



(a)



(b)

Figure 4. XRD spectra of (a) g-C₃N₄ nanosheets and (b) g-C₃N₄@L-arginine.

In Figure 5, $g\text{-C}_3\text{N}_4\text{@L-arginine}$ thermal stability was shown at the range from 50 to 800 °C. The weight ratio has decreased gradually from 100 to 200 °C because of the removal of absorbed water from $g\text{-C}_3\text{N}_4\text{@L-arginine}$. L-arginine's separation was observed from 200 to 400 °C. There is a dramatic decrease from 400 to 700 °C which is related to $g\text{-C}_3\text{N}_4$ nanosheet decomposition.

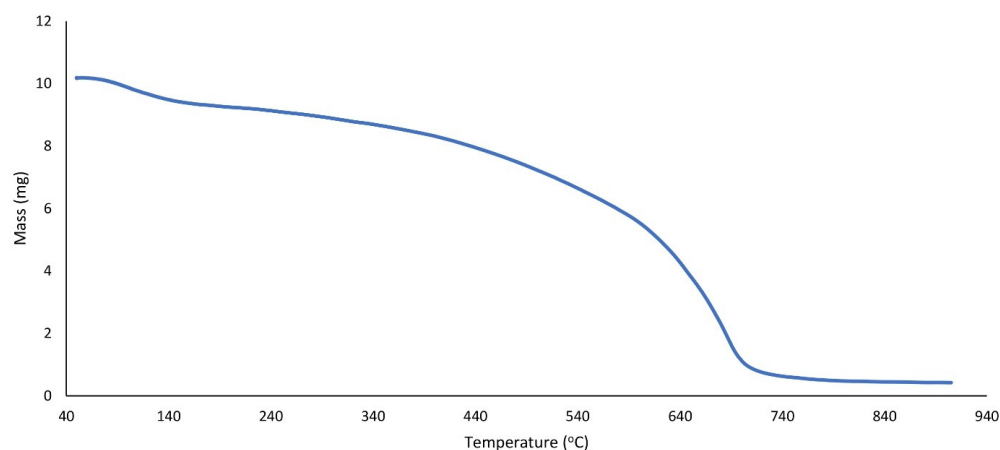


Figure 5. TGA spectrum of $g\text{-C}_3\text{N}_4\text{@L-arginine}$.

3.1. Application

The catalytic activity of produced heterogeneous nanocatalyst $g\text{-C}_3\text{N}_4\text{@L-arginine}$ was studied for multi-component reactions. The optimum reaction conditions for synthesizing acridinedione and pyranopyrazole derivatives were evaluated. The synthesis of acridinedione derivatives was performed by using dimedone (2 mmol), 4-chloro benzaldehyde (1 mmol), ammonium acetate (1 mmol), ethanol (5 mL), and catalyst (0.18 mol %) (model reaction 1). In addition, pyranopyrazole derivatives were produced by malononitrile (1.0 mmol), 4-chloro benzaldehyde (1.0 mmol), hydrazine hydrate (1.0 mmol), ethyl acetoacetate (1.0 mmol), ethanol (2.0 mL), and catalyst (0.18 mol %) (model reaction 2). The possibility of aldol reaction in aliphatic aldehydes would be the significant reason for using aromatic aldehydes compared to aliphatic aldehydes. Moreover, the reaction has been monitored by thin-layer chromatography (TLC). The model reactions have been investigated under different and convertible conditions. Initially, the reaction was performed with no catalyst at two different temperatures and the same reaction time (20 min). There was no acceptable efficiency as expected for both reactions (Table 1, entries 1–2). After using the catalyst (Table 1, entries 3–4), the desired products were produced in very small quantities at two different temperatures with the same environmental solvent. By using the catalyst at 80 °C for 20 min, there was a significant yield and efficiency of up to 92% for the first reaction and 91% for the second one (Table 1, entry 5). Moreover, despite increasing the reaction time up to 30 min, no noteworthy changes in the efficiency were observed (Table 1, entry 6).

In addition, changing the used solvent to water with the same condition as Table 1-entry 5 can decrease the efficiency of reactions 1 and 2 to 65% and 68%, respectively (Table 1, entry 7). If the solvent of the reactions changed to methanol and acetonitrile (Table 1, entries 8 and 9), the reaction yield, in comparison with entry 5, will be increased and decreased, respectively. Likewise, the model reactions were performed by $g\text{-C}_3\text{N}_4$ (0.18 mol %) and L-arginine (0.18 mol %) with the same conditions, while the yield of the final products was decreased.

After optimization, different aromatic aldehydes were used to show the merits of $g\text{-C}_3\text{N}_4\text{@L-arginine}$ catalytic activity and different pyranopyrazole and acridinedione derivatives were synthesized (Tables 2 and 3).

Table 1. Optimization of g-C₃N₄@L-arginine for reaction 1 and 2.

Entry	Catalyst	Temperature (°C)	Time (min)	Solvent	Yield (%) (Reaction 1)	Yield (%) (Reaction 2)
1	-	80	20	EtOH	-	-
2	-	80	20	EtOH	-	-
3	g-C ₃ N ₄ @L-arginine	RT	20	EtOH	12	14
4	g-C ₃ N ₄ @L-arginine	40	20	EtOH	53	48
5	g-C ₃ N ₄ @L-arginine	80	20	EtOH	92	91
6	g-C ₃ N ₄ @L-arginine	80	30	EtOH	90	87
7	g-C ₃ N ₄ @L-arginine	80	20	Water	65	68
8	g-C ₃ N ₄ @L-arginine	80	20	MeOH	86	73
9	g-C ₃ N ₄ @L-arginine	80	20	Acetonitrile	65	61
10	g-C ₃ N ₄	80	30	EtOH	Trace	Trace
11	L-arginine	80	30	EtOH	32	30

Table 2. Synthesis acridinedione derivatives by g-C₃N₄@L-arginine ^(a,b).

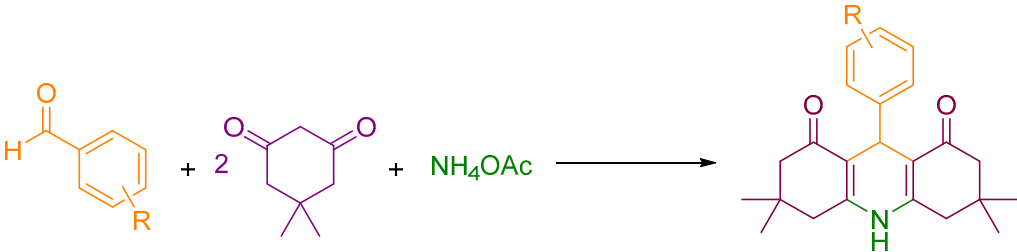
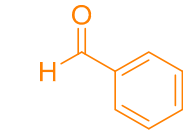
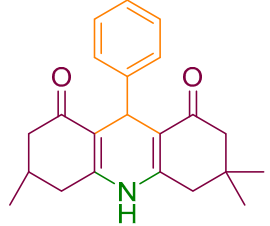
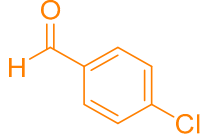
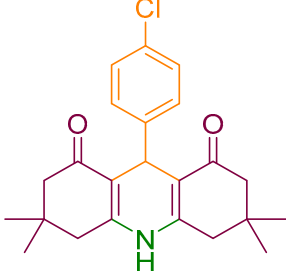
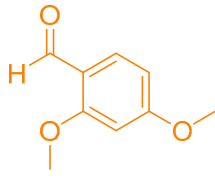
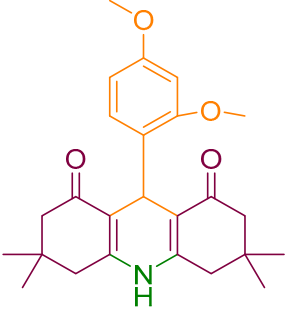
Entry	R	Amine	Product	Mp (°C, [Ref])	Yield (%)
					
1a		NH ₄ OAc		280–282 [35]	88
2a		NH ₄ OAc		302–304 [36]	92
3a		NH ₄ OAc		244–245 [37]	80

Table 2. Cont.

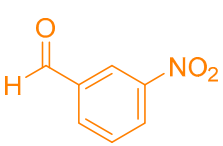
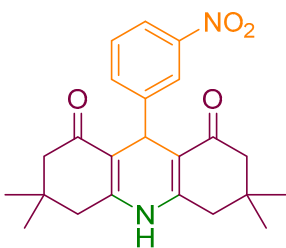
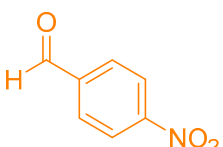
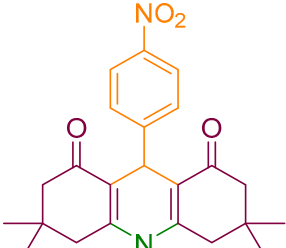
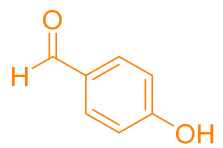
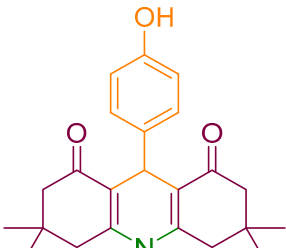
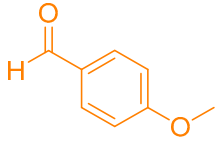
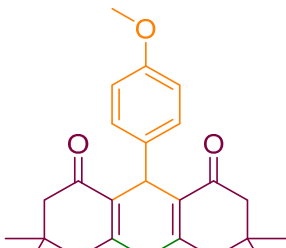
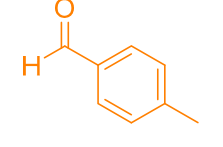
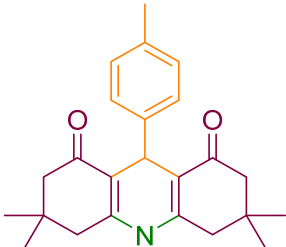
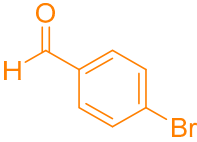
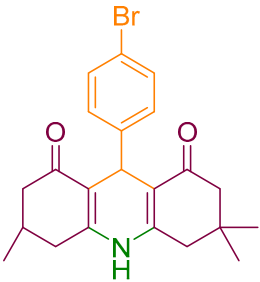
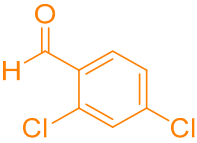
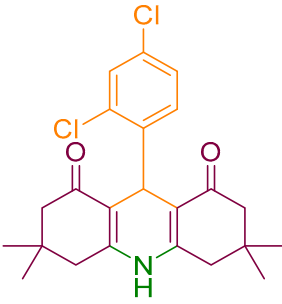
Entry	R	Amine	Product	Mp (°C, [Ref])	Yield (%)
4a		NH ₄ OAc		291–293 [38]	83
5a		NH ₄ OAc		299–300 [39]	85
6a		NH ₄ OAc		283–285 [40]	79
7a		NH ₄ OAc		271–273 [41]	87
8a		NH ₄ OAc		330–333 [42]	78

Table 2. Cont.

Entry	R	Amine	Product	Mp (°C, [Ref])	Yield (%)
9a		NH ₄ OAc		240–242 [43]	88
10a		NH ₄ OAc		319–321 [35]	90

^(a) Reaction conditions: aromatic aldehyde (1 mmol), dimedone (2 mmol), ammonium acetate (1 mmol), catalyst (20 mg), and ethanol (5 mL) refluxed in 80 °C. ^(b) Yields referred to pure products.

Table 3. Synthesis pyranopyrazole derivatives by g-C₃N₄@L-arginine ^(a,b).

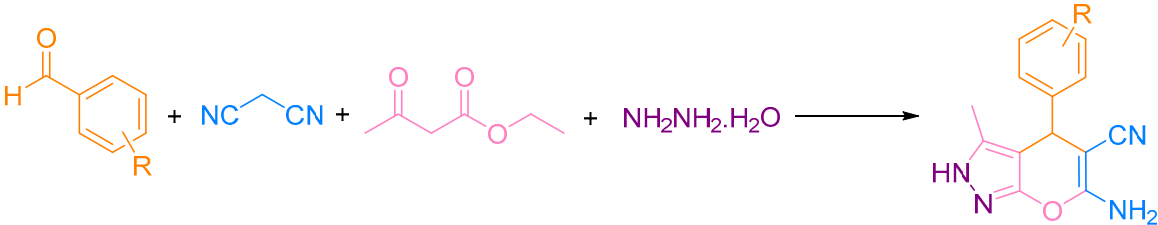
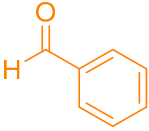
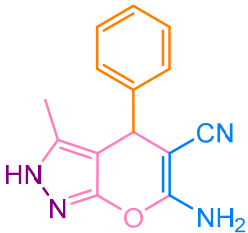
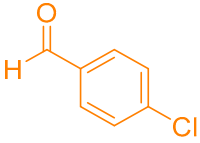
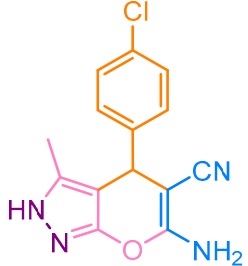
Entry	R	Product	Mp (°C, [Ref])	Yield (%)
				
1b			244–245 [44]	87
2b			227–229 [45]	91

Table 3. Cont.

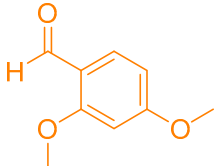
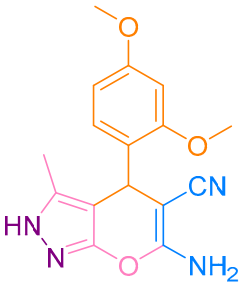
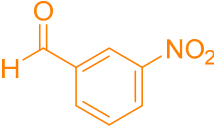
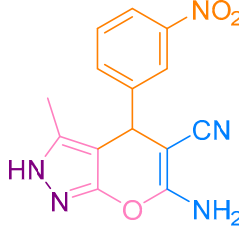
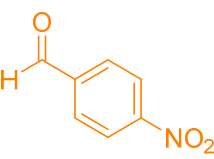
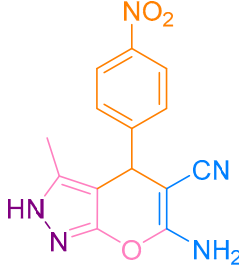
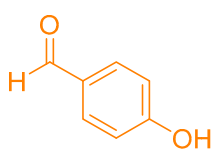
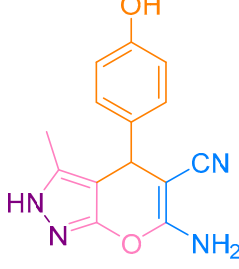
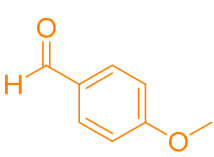
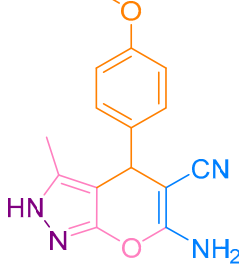
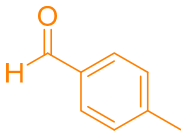
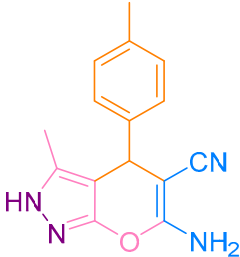
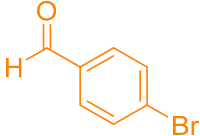
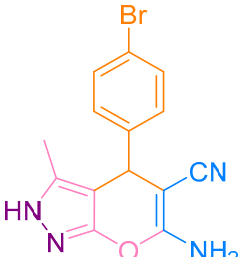
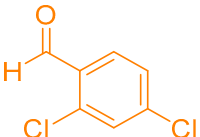
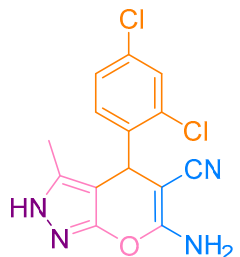
Entry	R	Product	Mp (°C, [Ref])	Yield (%)
3b			185–187 [46]	78
4b			237–238 [47]	83
5b			250–251 [48]	87
6b			225–227 [49]	76
7b			211–213 [19]	80

Table 3. Cont.

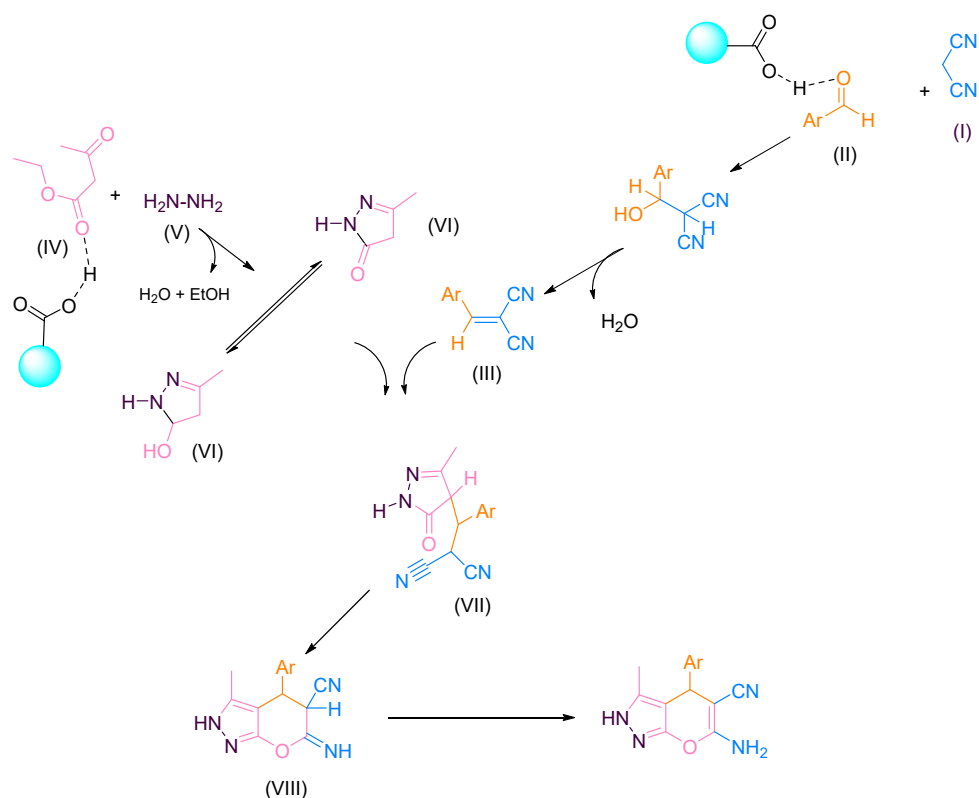
Entry	R	Product	Mp (°C, [Ref])	Yield (%)
8b			208–210 [49]	77
9b			184–186 [45]	84
10b			197–198 [50]	89

^(a) Reaction conditions: aromatic aldehyde (1 mmol), hydrazine hydrate (1 mmol), ethyl acetoacetate (1 mmol), malononitrile (1 mmol) catalyst (20 mg), and ethanol (5 mL) refluxed in 80 °C. ^(b) Yields referred to pure products.

3.2. Mechanism of Using Nanocatalyst for Synthesizing Pyranopyrazole and Acridinedione Derivatives

3.2.1. Pyranopyrazoles

The study of the mechanism for pyranopyrazole derivatives and the proposed mechanism is shown in Scheme 2. In addition, *g*-C₃N₄@L-arginine is needed for activating different intermediates and reactants. Malononitrile (I) and aromatic aldehyde (II) would react with each other by the carbon as a nucleophile. Then, it would react with the carbonyl group by releasing water and produce intermediate (III). Simultaneously, ethyl acetoacetate (IV) and hydrazine hydrate (V) react with each other and form the intermediate (VI). Afterward, the amine group's non-bonding electron pair reacts with the ethyl acetoacetate's carbonyl group. In the following step, the 5-member ring was closed by removing the water molecule. In the last step, two produced intermediates, ((III) and (VI)), would react with each other, and the pyranopyrazole derivative was synthesized.



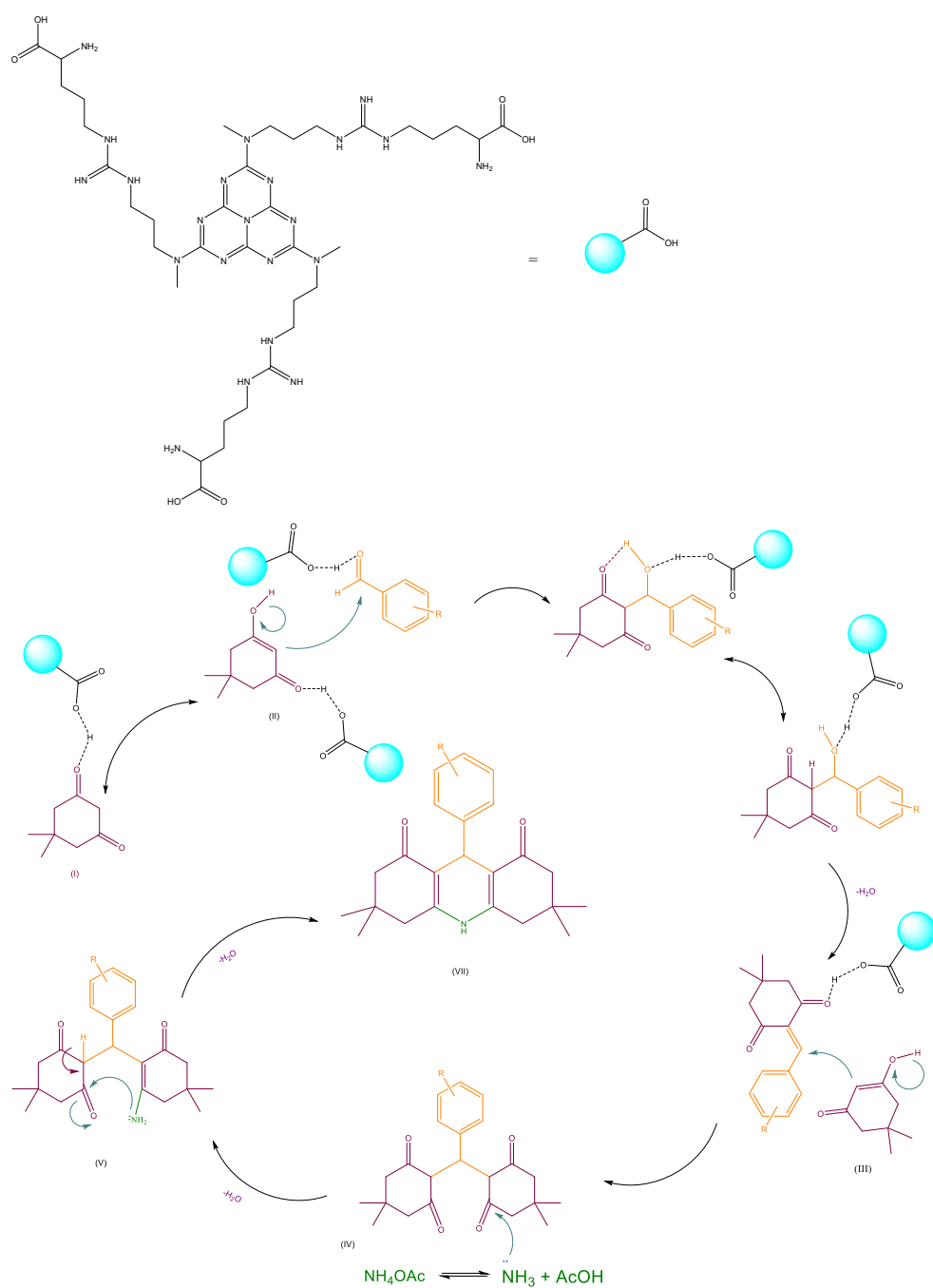
Scheme 2. Proposed mechanism for synthesizing pyranopyrazole derivatives.

3.2.2. Acridinediones

The study of the mechanism for acridinedione derivative synthesis and the proposed mechanism is exhibited in Scheme 3. For activating the carbonyl group of aldehydes, the presence of $g\text{-C}_3\text{N}_4@L\text{-arginine}$ is essential. After activating the carbonyl group with nanocatalyst (I) and producing the hydroxyl group on dimedone (II), the carbon nucleophile would react with activated aromatic aldehyde. Then, the other dimedone reacts with the double bond for donating electrons (III), and after a water molecule removal, the ring is closed by an intramolecular reaction (IV, V and VI). Eventually, the intended product is obtained (VII).

3.3. Reusability

The recovery and recyclability of the catalyst are the essential principles of green chemistry. Therefore, the reusability of $g\text{-C}_3\text{N}_4@L\text{-arginine}$ was studied for synthesizing pyranopyrazole and acridinedione derivatives. $g\text{-C}_3\text{N}_4@L\text{-arginine}$ was extracted from the reaction, washed with water and ethanol, then dried at 70°C . It was repeated 5 times in the same conditions. After each reaction, the yield decreased gradually, but it was acceptable (Figure 6).



Scheme 3. Proposed mechanism for synthesizing acridinedione derivatives.

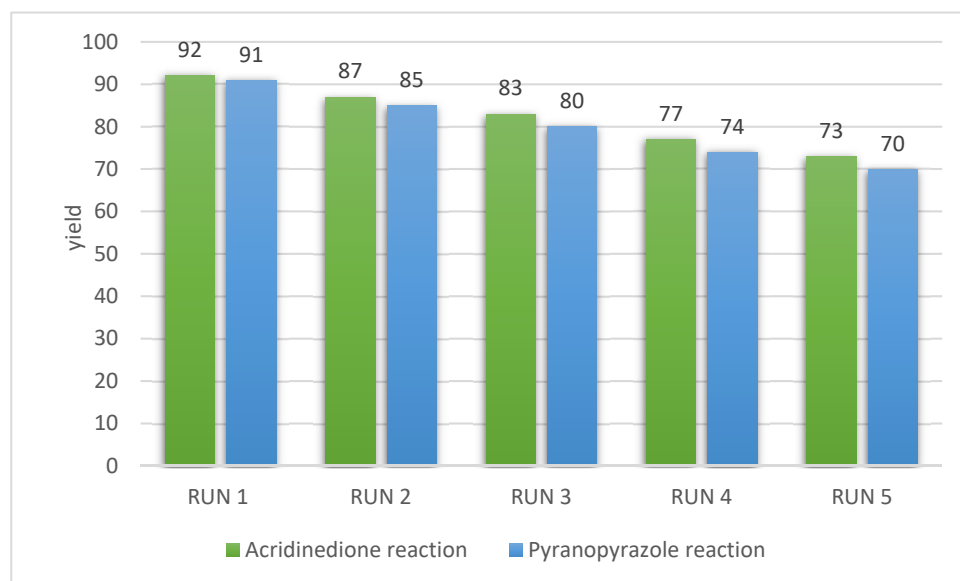


Figure 6. Reusability of $g\text{-C}_3\text{N}_4@L\text{-arginine}$ in acridinedione and pyranopyrazole derivatives.

4. Conclusions

In conclusion, in this project, we utilized an easy and convenient method for preparing $g\text{-C}_3\text{N}_4@L\text{-arginine}$ nanocatalyst and applied it for producing pyranopyrazole and acridinedione derivatives. $G\text{-C}_3\text{N}_4@L\text{-arginine}$ nanocatalyst has remarkable advantages such as reusability, easy separation, high efficiency, and short reaction time. According to the results, produced nanocatalyst is the superior compared to other reported catalysts.

Author Contributions: Conceptualization, supervision, validation, H.G.; investigation, Z.T.; methodology, P.H., M.T. and Z.T.; writing—review and editing, writing—original draft preparation, H.G., P.H. and F.B. All authors have read and agreed to the published version of the manuscript.

Funding: This research received no external funding.

Institutional Review Board Statement: Not applicable.

Informed Consent Statement: Not applicable.

Data Availability Statement: Not applicable.

Conflicts of Interest: The authors declare no conflict of interest.

References

- Swain, S.; Altaee, A.; Saxena, M.; Samal, A.K. A comprehensive study on heterogeneous single atom catalysis: Current progress, and challenges. *Coord. Chem. Rev.* **2022**, *470*, 214710. [[CrossRef](#)]
- Zhi, Y.; Wang, Z.; Zhang, H.; Zhang, Q. Recent progress in metal-free covalent organic frameworks as heterogeneous catalysts. *Small* **2020**, *16*, 2001070. [[CrossRef](#)] [[PubMed](#)]
- Ghafuri, H.; Tajik, Z.; Ghanbari, N.; Hanifehnejad, P. Preparation and characterization of graphitic carbon nitride-supported L-arginine as a highly efficient and recyclable catalyst for the one-pot synthesis of condensation reactions. *Sci. Rep.* **2021**, *11*, 19792. [[CrossRef](#)] [[PubMed](#)]
- Ghafuri, H.; Rashidizadeh, A. Facile preparation of $\text{CuS-g-C}_3\text{N}_4/\text{Ag}$ nanocomposite with improved photocatalytic activity for the degradation of rhodamine B. *Polyhedron* **2020**, *179*, 114368. [[CrossRef](#)]
- Akhtar, B.; Ghafuri, H.; Rashidizadeh, A. Synergistic effect of iodine doped TiO_2 nanoparticle/ $g\text{-C}_3\text{N}_4$ nanosheets with upgraded visible-light-sensitive performance toward highly efficient and selective photocatalytic oxidation of aromatic alcohols under blue LED irradiation. *Mol. Catal.* **2021**, *506*, 111527. [[CrossRef](#)]
- Rahmati, M.; Ghafuri, H. Catalytic Strecker reaction: $G\text{-C}_3\text{N}_4$ -anchored sulfonic acid organocatalyst for the synthesis of α -aminonitriles. *Res. Chem. Intermed.* **2021**, *47*, 1489–1502. [[CrossRef](#)]
- Rashidizadeh, A.; Ghafuri, H.; Rezazadeh, Z. Improved visible-light photocatalytic activity of $g\text{-C}_3\text{N}_4/\text{CuWO}_4$ nanocomposite for degradation of methylene blue. *Multidiscip. Digit. Publ. Inst. Proc.* **2020**, *41*, 43.

8. Rashidizadeh, A.; Ghafuri, H. g-C₃N₄/Ni nanocomposite: An efficient and eco-friendly recyclable catalyst for the synthesis of quinoxalines. *Multidiscip. Digit. Publ. Inst. Proc.* **2019**, *9*, 49.
9. Singh, L.; Shrivastav, A.; Verma, N. Effect of L-arginine amino acid on liver regeneration after hepatocyte damage in rats: An experimental study. *J. Drug Deliv. Ther.* **2019**, *9*, 470–476.
10. Hamzavi, S.F.F.; Jamili, S.; Yousefzadi, M.; Moradi, A.M.; Biuki, N.A. Silver nanoparticles supported on chitosan as a green and robust heterogeneous catalyst for direct synthesis of nitrogen heterocyclic compounds under green conditions. *Bull. Chem. React. Eng. Catal.* **2019**, *14*, 51–59. [[CrossRef](#)]
11. Kamalzare, M.; Ahghari, M.R.; Bayat, M.; Maleki, A. Fe₃O₄@chitosan-tannic acid bionanocomposite as a novel nanocatalyst for the synthesis of pyranopyrazoles. *Sci. Rep.* **2021**, *11*, 20021. [[CrossRef](#)]
12. Lin, Y.Y.; Hung, K.Y.; Liu, F.Y.; Dai, Y.M.; Lin, J.H.; Chen, C.C. Photocatalysts of quaternary composite, bismuth oxyfluoride/bismuth oxyiodide/graphitic carbon nitride: Synthesis, characterization, and photocatalytic activity. *Mol. Catal.* **2022**, *528*, 112463. [[CrossRef](#)]
13. Edrisi, M.; Azizi, N. Sulfonic acid-functionalized graphitic carbon nitride composite: A novel and reusable catalyst for the one-pot synthesis of polysubstituted pyridine in water under sonication. *J. Iran. Chem. Soc.* **2020**, *17*, 901–910. [[CrossRef](#)]
14. Nasiriani, T.; Javanbakht, S.; Nazeri, M.T.; Farhid, H.; Khodkari, V.; Shaabani, A. Isocyanide-Based Multicomponent Reactions in Water: Advanced Green Tools for the Synthesis of Heterocyclic Compounds. *Top. Curr. Chem.* **2022**, *380*, 50. [[CrossRef](#)]
15. Nandi, S.; Jamatia, R.; Sarkar, R.; Sarkar, F.K.; Alam, S.; Pal, A.K. One-Pot Multicomponent Reaction: A Highly Versatile Strategy for the Construction of Valuable Nitrogen-Containing Heterocycles. *ChemistrySelect* **2022**, *7*, e202201901. [[CrossRef](#)]
16. Farhid, H.; Khodkari, V.; Nazeri, M.T.; Javanbakht, S.; Shaabani, A. Multicomponent reactions as a potent tool for the synthesis of benzodiazepines. *Org. Biomol. Chem.* **2021**, *19*, 3318–3358. [[CrossRef](#)]
17. Goddard, J.-P.; Malacria, M.; Ollivier, C. *Multi-component Reactions in Molecular Diversity*; John Wiley & Sons: Hoboken, NJ, USA, 2020.
18. Becerra, D.; Abonia, R.; Castillo, J.-C. Recent Applications of the Multicomponent Synthesis for Bioactive Pyrazole Derivatives. *Molecules* **2022**, *27*, 4723. [[CrossRef](#)]
19. Wu, M.; Feng, Q.; Wan, D.; Ma, J. CTACl as catalyst for four-component, one-pot synthesis of pyranopyrazole derivatives in aqueous medium. *Synth. Commun.* **2013**, *43*, 1721–1726. [[CrossRef](#)]
20. Reddy, G.; Raul, J. Garcia Synthesis of Pyranopyrazoles under Eco-friendly Approach by Using Acid Catalysis. *J. Heterocycl. Chem.* **2017**, *54*, 89–94. [[CrossRef](#)]
21. Patil, U.; Patil, R.; Patil, S. An Eco-friendly Catalytic System for One-pot Multicomponent Synthesis of Diverse and Densely Functionalized Pyranopyrazole and Benzochromene Derivatives. *J. Heterocycl. Chem.* **2019**, *56*, 1898–1913. [[CrossRef](#)]
22. Nikoorazm, M.; Tahmasbi, B.; Gholami, S.; Moradi, P. Copper and nickel immobilized on cytosine@MCM-41: As highly efficient, reusable and organic–inorganic hybrid nanocatalysts for the homoselective synthesis of tetrazoles and pyranopyrazoles. *Appl. Organomet. Chem.* **2020**, *34*, e5919. [[CrossRef](#)]
23. Mukherjee, P.; Das, A. Spirocyclopropanes from Intramolecular Cyclopropanation of Pyranopyrazoles and Pyranopyrimidinediones and Lewis Acid Mediated (3 + 2) Cycloadditions of Spirocyclopropylpyrazolones. *J. Org. Chem.* **2017**, *82*, 2794–2802. [[CrossRef](#)] [[PubMed](#)]
24. Khandare, P.M.; Ingale, R.D.; Taware, A.S.; Shisodia, S.U.; Pawar, S.S.; Kotai, L.; Pawar, R.P. One pot synthesis and biological evaluation of pyranopyrazoles in aqueous medium. *Eur. Chem. Bull.* **2017**, *6*, 410–414. [[CrossRef](#)]
25. Madar, J.M.; Samundeeswari, S.; Holiyachi, M.; Naik, N.S.; Pawar, V.; Gudimani, P.; Shastri, L.A.; Kumbar, V.M.; Sunagar, V.A. Solvent-Free Synthesis, Characterization, and In Vitro Biological Activity Study of Xanthenediones and Acridinediones. *Russ. J. Bioorg. Chem.* **2021**, *47*, 535–542. [[CrossRef](#)]
26. Jamalian, A.; Miri, R.; Firuzi, O.; Amini, M.; Moosavi-Movahedi, A.A.; Shafieea, A. Synthesis, cytotoxicity and calcium antagonist activity of novel imidazolyl derivatives of 1,8-acridinediones. *J. Iran. Chem. Soc.* **2011**, *8*, 983–991. [[CrossRef](#)]
27. Alvala, M.; Bhatnagar, S.; Ravi, A.; Jeankumar, V.U.; Manjashetty, T.H.; Yogeewari, P.; Sriram, D. Novel acridinedione derivatives: Design, synthesis, SIRT1 enzyme and tumor cell growth inhibition studies. *Bioorg. Med. Chem. Lett.* **2012**, *22*, 3256–3260. [[CrossRef](#)]
28. Behbahani, F.S.; Tabeshpour, J.; Mirzaei, S.; Golmakaniyoon, S.; Tayarani-Najaran, Z.; Ghasemi, A.; Ghodsi, R. Synthesis and biological evaluation of novel benzo[*c*]acridine-diones as potential anticancer agents and tubulin polymerization inhibitors. *Arch. der Pharm.* **2019**, *352*, 1800307. [[CrossRef](#)]
29. Aday, B.; Yildiz, Y.; Ulus, R.; Eris, S.; Sen, F.; Kaya, M. One-pot, efficient and green synthesis of acridinedione derivatives using highly monodisperse platinum nanoparticles supported with reduced graphene oxide. *New J. Chem.* **2016**, *40*, 748–754. [[CrossRef](#)]
30. Ulus, R.; Yildiz, Y.; ERİŞ, S.; Aday, B.; Sen, F.; Kaya, M. Functionalized multi-walled carbon nanotubes (f-MWCNT) as highly efficient and reusable heterogeneous catalysts for the synthesis of acridinedione derivatives. *ChemistrySelect* **2016**, *1*, 3861–3865. [[CrossRef](#)]
31. Xia, J.-J.; Zhang, K.-H. Synthesis of N-substituted acridinediones and polyhydroquinoline derivatives in refluxing water. *Molecules* **2012**, *17*, 5339–5345. [[CrossRef](#)]
32. Zhu, A.; Liu, R.; Du, C.; Li, L. Betainium-based ionic liquids catalyzed multicomponent Hantzsch reactions for the efficient synthesis of acridinediones. *RSC Adv.* **2017**, *7*, 6679–6684. [[CrossRef](#)]

33. Mansoor, S.S.; Aswin, K.; Logaiya, K.; Sudhan, S. Aqua-mediated synthesis of acridinediones with reusable silica-supported sulfuric acid as an efficient catalyst. *J. Taibah Univ. Sci.* **2014**, *8*, 265–275. [[CrossRef](#)]
34. Qiu, P.; Chen, H.; Xu, C.; Zhou, N.; Jiang, F.; Wang, X.; Fu, Y. Fabrication of an exfoliated graphitic carbon nitride as a highly active visible light photocatalyst. *J. Mater. Chem. A* **2015**, *3*, 24237–24244. [[CrossRef](#)]
35. Taheri-Ledari, R.; Esmaili, M.S.; Varzi, Z.; Eivazzadeh-Keihan, R.; Maleki, A.; Shalan, A.E. Facile route to synthesize Fe₃O₄@acacia-SO₃H nanocomposite as a heterogeneous magnetic system for catalytic applications. *RSC Adv.* **2020**, *10*, 40055–40067. [[CrossRef](#)]
36. Zolfigol, M.A.; Karimi, F.; Yarie, M.; Torabi, M. Catalytic application of sulfonic acid-functionalized titania-coated magnetic nanoparticles for the preparation of 1,8-dioxodecahydroacridines and 2,4,6-triarylpyridines via anomeric-based oxidation. *Appl. Organomet. Chem.* **2018**, *32*, e4063. [[CrossRef](#)]
37. Mahesh, P.; Guruswamy, K.; Diwakar, B.S.; Devi, B.R.; Murthy, Y.L.N.; Kollu, P.; Pammi, S.V.N. Magnetically separable recyclable nano-ferrite catalyst for the synthesis of acridinediones and their derivatives under solvent-free conditions. *Chem. Lett.* **2015**, *44*, 1386–1388. [[CrossRef](#)]
38. Kiani, M.; Mohammadipour, M. Fe₃O₄@SiO₂-MoO₃H nanoparticles: A magnetically recyclable nanocatalyst system for the synthesis of 1,8-dioxo-decahydroacridine derivatives. *RSC Adv.* **2017**, *7*, 997–1007. [[CrossRef](#)]
39. Aher, D.; Khillare, K.; Shankarwar, S. Incorporation of Keggin-based H₃PW₇Mo₅O₄₀ into bentonite: Synthesis, characterization and catalytic applications. *RSC Adv.* **2021**, *11*, 11244–11254. [[CrossRef](#)]
40. Bazdid-Vahdaty, N.; Mamaghani, M.; Khalili, B.; Tavakoli, F. Ag/CuO/MCM-48 AS A potential CATALYST for the synthesis of symmetrical and unsymmetrical polyhydroquinolines. *J. Chil. Chem. Soc.* **2021**, *66*, 5136–5141. [[CrossRef](#)]
41. Alponi, L.H.; Picinini, M.; Urquieta-Gonzalez, E.A.; Corrêa, A.G. USY-zeolite catalyzed synthesis of 1,4-dihydropyridines under microwave irradiation: Structure and recycling of the catalyst. *J. Mol. Struct.* **2021**, *1227*, 129430. [[CrossRef](#)]
42. Hasannezhad, N.; Shadjou, N. KCC-1-nPr-NH-Arg as an efficient organo-nanocatalyst for the green synthesis of 1,8-dioxo decahydroacridine derivatives. *J. Mol. Recognit.* **2022**, *35*, e2956. [[CrossRef](#)] [[PubMed](#)]
43. Khojastehnezhad, A.; Rahimizadeh, M.; Eshghi, H.; Moeinpour, F.; Bakavoli, M. Ferric hydrogen sulfate supported on silica-coated nickel ferrite nanoparticles as new and green magnetically separable catalyst for 1,8 dioxodecahydroacridine synthesis. *Chin. J. Catal.* **2014**, *35*, 376–382. [[CrossRef](#)]
44. Hojati, S.F.; Amiri, A.; MoeiniEghbali, N.; Mohamadi, S. Polypyrrole/Fe₃O₄/CNT as a recyclable and highly efficient catalyst for one-pot three-component synthesis of pyran derivatives. *Appl. Organomet. Chem.* **2018**, *32*, e4235. [[CrossRef](#)]
45. Heravi, M.M.; Malakooti, R.; Kafshdarzadeh, K.; Amiri, Z.; Zadsirjan, V.; Atashin, H. Supported palladium oxide nanoparticles in Al-SBA-15 as an efficient and reusable catalyst for the synthesis of pyranopyrazole and benzylpyrazolyl coumarin derivatives via multicomponent reactions. *Res. Chem. Intermed.* **2022**, *48*, 203–234. [[CrossRef](#)]
46. Maleki, A.; Eskandarpour, V. Design and development of a new functionalized cellulose-based magnetic nanocomposite: Preparation, characterization, and catalytic application in the synthesis of diverse pyrano [2,3-*c*] pyrazole derivatives. *J. Iran. Chem. Soc.* **2019**, *16*, 1459–1472. [[CrossRef](#)]
47. Abdolahi, S.; Hajjami, M.; Gholamian, F. An approach to the synthesis and characterization of HMS/Pr-Rh-Zr as efficient catalyst for synthesis of tetrahydrobenzo[*b*]pyran and 1,4-dihydropyrano[2,3-*c*]pyrazole derivatives. *Res. Chem. Intermed.* **2021**, *47*, 1883–1904. [[CrossRef](#)]
48. Kumari, R.; Varghese, A.; George, L.; Akshaya, K.B. Photophysical study of 6-amino-3-methyl-4-(4-nitrophenyl)-1,4-dihydropyrano[2,3-*c*]pyrazole-5-carbonitrile and estimation of ground-state and singlet excited-state dipole moments by solvatochromic approaches. *J. Mol. Liq.* **2016**, *222*, 828–835. [[CrossRef](#)]
49. Shaterian, H.; Azizi, K. Mild, four-component synthesis of 6-amino-4-aryl-3-methyl-1,4-dihydropyrano[2, 3-*c*]pyrazole-5-carbonitriles catalyzed by titanium dioxide nano-sized particles. *Res. Chem. Intermed.* **2014**, *40*, 661–667. [[CrossRef](#)]
50. Hassanzadeh-Afruzi, F.; Dogari, H.; Esmailzadeh, F.; Maleki, A. Magnetized melamine-modified polyacrylonitrile (PAN@ melamine/Fe₃O₄) organometallic nanomaterial: Preparation, characterization, and application as a multifunctional catalyst in the synthesis of bioactive dihydropyrano[2,3-*c*]pyrazole and 2-amino-3-cyano 4H-pyran derivatives. *Appl. Organomet. Chem.* **2021**, *35*, e6363.